View metadata, citation and similar papers at core.ac.uk
brought to you by CORE
provided by NASA Technical Reports Server

Technical Report No. 32-173

Interplanetary Trajectory Optimization With Power-Limited Propulsion Systems

W. G. Melbourne
D. E. Richardson
C. G. Sauer

JET PROPULSION LABORATORY
CALIFORNIA INSTITUTE OF TECHNOLOGY
PASADENA, CALIFORNIA

February 26, 1962

NATIONAL AERONAUTICS AND SPACE ADMINISTRATION
CONTRACT NO. NAS 7-100

Technical Report No. 32-173

Interplanetary Trajectory Optimization With Power-Limited Propulsion Systems

W. G. Melbourne
D. E. Richardson
C. G. Sauer

C. R. Gates

C. R. Gates, Chief
Systems Anaylsis

JET PROPULSION LABORATORY
CALIFORNIA INSTITUTE OF TECHNOLOGY
PASADENA, CALIFORNIA

February 26, 1962

Copyright © 1962
Jet Propulsion Laboratory
California Institute of Technology

CONTENTS

I. Introduction 1

II. Optimum-Thrust Equations 2

III. Optimization Criteria 6

IV. Interplanetary Rendezvous Trajectories 8

V. Three-Dimensional Rendezvous Trajectories 10

VI. Interplanetary Round-Trip Trajectories 11

VII. Round-Trip Trajectory Calculations for an Earth-to-Mars Mission 12

VIII. A Three-Dimensional Example of a 1971–1972 Mars Round-Trip Mission 14

References 17

Appendix 18

TABLES

1. Comparison of vehicle performance 5

2. Comparison of $\int a^2 dt$ for exhaust velocities of 50,000 m/sec and ∞ . . . 9

3. Comparison of $\int a^2 dt$ for three-dimensional example and example using coplanar, circular end conditions 15

PRECEDING PAGE BLANK NOT FILMED

Preceding page blank

FIGURES

1. Thrust-mode transfer sequence, 184-day Mars trajectory 5

2. Exhaust velocity vs time, 184-day Mars trajectory 5

3. $\int a^2 dt$ vs flight time, Martian rendezvous trajectories 9

4. $\int a^2 dt$ vs flight time, Venusian rendezvous trajectories 9

5. $\int a^2 dt$ vs launch date; 120-, 184-, and 360-day Martian rendezvous trajectories during 1970–71 10

6. Contours of equal $\int a^2 dt$, flight time vs launch date for Martian rendezvous trajectories during 1970–71 10

7. $\int a^2 dt$ vs launch date, 544-day Martian round trip with circular end conditions 12

8. Earth-to-Mars transfer trajectory, 184-day flight time, ecliptic projection 14

9. Mars-to-Earth transfer trajectory, 312-day flight time, ecliptic projection 14

10. Exhaust velocity vs time, 544-day Martian round trip 15

11. Normalized vehicle mass vs time, 544-day Martian round trip 16

A-1. Search procedure 19

PRECEDING PAGE BLANK NOT FILMED.

Preceding page blank

PREFACE

This paper was presented at the Institute of Aerospace Sciences Specialists Meeting on Vehicle Systems Optimization, Garden City, New York, November 28–29, 1961.

PRECEDING PAGE BLANK NOT FILMED

Preceding page blank

ABSTRACT

A trajectory-optimization process is described in which the optimum-thrust equations are derived using the calculus of variations. The magnitude of the thrust is constrained within an upper and a lower bound, but the thrust direction is arbitrary. This formulation allows both the constant-thrust program and the variable-thrust program to be considered. For the constant-thrust program, certain propulsion-system parameters are optimized for maximum final vehicle mass. This theory has been used to study interplanetary missions to Venus and Mars using a power-limited propulsion system. Both one-way and round-trip rendezvous trajectories are considered. The analysis employs a two-body inverse-square force-field model of three dimensions. An iterative routine used to solve the two-point boundary-value problem is described in the Appendix.

I. INTRODUCTION

This Report presents the results of a systematic investigation of the payload capability of power-limited low-thrust vehicles for various interplanetary missions. The analysis is based upon a two-body inverse-square force field model of three dimensions in which the trajectory is optimized in the sense of maximizing or minimizing some terminal quantity such as time or vehicle payload while simultaneously satisfying other specified terminal quantities.

Two thrust programs are described which bracket that class of trajectories and vehicle performances that an actual vehicle would be capable of achieving. These thrust programs are characterized by either a constant exhaust velocity of the expellants and hence, constant thrust, or by an exhaust velocity that is unconstrained in magnitude, the latter program giving rise to the so-called optimum-thrust equations of power-limited flight (Refs. 1, 2) and yielding the absolute maximum payload the vehicle may have for a given power level. For a particular mission, the generation of a pair of trajectories using the two thrust programs is extremely valuable in the determination of mission feasibility, payload capability, and trajectory design.

The optimization of the trajectory is accomplished by a calculus-of-variations method in which a terminal quantity is maximized or minimized subject to prescribed boundary conditions and certain constraints; namely, the equations of motion and the thrust program. An iterative routine is used to solve the two-point boundary-value problem in order to obtain numerical solutions for specified terminal conditions.

The results of this investigation include the generation of optimum rendezvous and round-trip trajectories for a typical mission to Mars. A comparison of the results obtained from an analysis of transfer between coplanar circular orbits assumed for the Earth and Mars and the results of an analysis of the transfer between the actual three-dimensional orbits of the Earth and Mars is also mentioned.

II. OPTIMUM-THRUST EQUATIONS

The problem of optimizing the trajectory of an interplanetary vehicle is very conveniently treated as a calculus-of-variations problem of the Mayer type, in which a function of the generalized coordinates of the endpoints of the trajectory

$$J = J\,[q_j(t_1), q_j(t_0), t_1] \tag{1}$$

is extremalized subject to certain boundary conditions and certain constraints; namely, the equations of motion, the thrust program constraints, etc. The constraining equations are

$$\dot{\mathbf{v}} + \nabla U - \mathbf{a} = 0 \tag{2}$$

$$\mathbf{v} - \dot{\mathbf{r}} = 0 \tag{3}$$

$$a - \frac{\beta}{c}\frac{\alpha_p}{\mu} = 0 \tag{4}$$

$$\dot{\mu} + \frac{\beta}{c^2}\alpha_p = 0 \tag{5}$$

Equations (2) and (3) are the equations of motion, where $\mathbf{r}$ is the position vector of the vehicle and U is the potential of the force field. The thrust acceleration is defined by Eq. (4), in which μ is the normalized vehicle mass and α_p is a normalized power parameter ranging between a value of unity (maximum power) and zero (coasting), as will be shown subsequently. The bounds on α_p may be expressed in analytic form through the equality constraint

$$\gamma^2 - \alpha_p(1 - \alpha_p) = 0 \tag{6}$$

where γ is defined to be a real variable. The quantity β appearing in Eqs. (4) and (5) is twice the maximum power in the rocket exhaust per unit initial mass of the vehicle and is, therefore, a constant determined by the engineering design. The quantity c appearing in these equations is the rocket exhaust velocity of the expellants, which is either continuously variable or constant, depending upon the thrust program used. Equation (5) is the normalized differential form for the rocket mass.

Both the variable- and constant-thrust programs may be solved by a consideration of a more general thrust program containing both of these modes, in which c is allowed to vary between two bounds. As before, these bounds may be expressed in terms of an equality constraint of the form

$$\eta^2 - (c_{\max} - c)(c - c_{\min}) = 0 \tag{7}$$

where η is defined as a real variable. By solving the calculus-of-variations problem with this additional equality constraint, the optimum-thrust equations for the programs under discussion are obtained quite simply by setting $c_{\min} = 0$ and $c_{\max} = \infty$ for the first case and by setting $c_{\min} = c_{\max} =$ constant for the second case.

A Mayer formulation (Ref. 3) has been applied to this more general problem to obtain the optimum-thrust equations. The present treatment is similar to that followed by Miele (Ref. 4), Lawden (Ref. 5), Leitmann (Ref. 6), and others.

Let $q_j(t)$ denote both the state and the control variables of the problem $(j = 1, 2, \cdots, n)$. Let the constraining relations be denoted by the functions

$$G_i(q_j, \dot{q}_j, t) = 0 \qquad i = 1, 2, \cdots, m < n \tag{8}$$

and let $\lambda_i(t)$ be a set of time-dependent Lagrange multipliers. Let F be a function defined by

$$F = \lambda_i G_i \tag{9}$$

where the summation rule is employed. As necessary conditions for extremizing J, the q_j must satisfy the Euler–Lagrange equations given by

$$\frac{d}{dt}\frac{\partial F}{\partial \dot{q}_j} - \frac{\partial F}{\partial q_j} = 0 \qquad j = 1, 2, \cdots, n \tag{10}$$

at all points along the trajectory except at corners; i.e., points of discontinuity in one or more of the q_j. Further, at such corners, the Weierstrass–Erdmann corner conditions must hold; namely,

$$\frac{\partial F}{\partial \dot{q}_j} \text{ is continuous} \qquad j = 1, 2, \cdots, n \tag{11}$$

$$F - \frac{\partial F}{\partial \dot{q}_j}\dot{q}_j \text{ is continuous} \tag{12}$$

If the constraining functions are not explicit functions of time, a first integral of the Euler–Lagrange equations is

$$F - \frac{\partial F}{\partial \dot{q}_j}\dot{q}_j = \text{constant} \tag{13}$$

One additional tool from the calculus-of-variations will be needed in dealing with corners; namely, the Weierstrass E-function. This function yields a further necessary condition for the minimization of J by the inequality

$$E = F(q_j^*, \dot{q}_j^*) - F(q_j, \dot{q}_j) - \sum_{k=1}^{n} (\dot{q}_k^* - \dot{q}_k)\frac{\partial F}{\partial \dot{q}_k} \geqq 0 \tag{14}$$

The q_j^* is an admissible value in the vicinity of q_j. For continuous variables, $q_j^* = q_j$; however, for discontinuous variables, q_j^* may take on any value consistent with the specified bounds.

In three dimensions, Eqs. (2) to (7) form a system of ten constraining relations which must be included in the optimization process. There are in this formulation fourteen variables, of which $\mathbf{v}$, $\mathbf{r}$, and μ are the state variables; α_p, c, and $\mathbf{a}$ are the control variables, with the latter being related through Eq. (4); and the quantities η and γ are auxiliary variables. In this problem, G_1, G_2, and G_3 are the equations of motion contained in Eq. (2); the functions G_7, G_8, G_9, and G_{10} are Eqs. (4), (5), (6), and (7), respectively.

The Euler–Lagrange equations for this problem are given by the relations

$$\mathbf{v}, \mathbf{r}: \ddot{\boldsymbol{\lambda}} + (\boldsymbol{\lambda}\cdot\nabla)\nabla U = 0 \tag{15}$$

$$\mathbf{a}: \mathbf{l}\cdot\boldsymbol{\lambda} - \lambda_7 = 0 \tag{16}$$

or

$$\boldsymbol{\lambda} - \mathbf{l}\lambda_7 = 0 \tag{16a}$$

$$\mu: \dot{\lambda}_8 - \frac{\beta\alpha_p}{c\mu^2}\lambda_7 = 0 \tag{17}$$

$$c: \frac{\beta}{c^2}\alpha_p\left(\frac{\lambda_7}{\mu} - \frac{2\lambda_8}{c}\right) + \lambda_{10}(2c - c_{\min} - c_{\max}) = 0 \tag{18}$$

$$\alpha_p: \frac{\beta}{c}\left(\frac{\lambda_7}{\mu} - \frac{\lambda_8}{c}\right) - \lambda_9(2\alpha_p - 1) = 0 \tag{19}$$

$$\gamma: \gamma\lambda_9 = 0 \tag{20}$$

$$\eta: \eta\lambda_{10} = 0 \tag{21}$$

where the vector $\mathbf{l}$ is the unit thrust vector and is equal to $\mathbf{a}/a$. The vector $\boldsymbol{\lambda}$ is the vector sum of the three orthogonal quantities λ_1, λ_2, and λ_3, the magnitude of $\boldsymbol{\lambda}$ hereafter being denoted by λ.

Since the potential U is assumed to be explicitly independent of time, the Euler equations admit a first integral of the form

$$\dot{\boldsymbol{\lambda}}\cdot\mathbf{v} + \boldsymbol{\lambda}\cdot\nabla U - \frac{\beta}{c}\alpha_p\left(\frac{\mathbf{l}\cdot\boldsymbol{\lambda}}{\mu} - \frac{\lambda_8}{c}\right) = \text{constant} = K_2 \tag{22}$$

where λ_7 has been replaced by $\mathbf{l}\cdot\boldsymbol{\lambda}$. Now, an application of the Weierstrass–Erdmann corner conditions yields the following summary:

(1) Continuous variables: $\mathbf{r}$, $\mathbf{v}$, μ

(2) Possibly discontinuous variables: $\mathbf{l}$, $\dot{\mu}$, c, γ, η, and α_p

(3) Continuous Lagrange multipliers: $\boldsymbol{\lambda}$, $\dot{\boldsymbol{\lambda}}$, λ_8

In view of the continuity considerations above, the Weierstrass E-function becomes

$$E = \frac{\alpha_p}{c}\left(\frac{\mathbf{l}\cdot\boldsymbol{\lambda}}{\mu} - \frac{\lambda_8}{c}\right) - \frac{\alpha_p^*}{c}\left(\frac{\mathbf{l}^*\cdot\boldsymbol{\lambda}}{\mu} - \frac{\lambda_8}{c^*}\right) \geqq 0 \tag{23}$$

Since condition (23) holds for all admissible values of the pertinent variables, it holds, in particular, when $\alpha_p = \alpha_p^*$ and $c = c^*$; thus,

$$(\mathbf{l}\cdot\boldsymbol{\lambda}) - (\mathbf{l}^*\cdot\boldsymbol{\lambda}) \geqq 0 \tag{24}$$

In order for (24) to be true, $\mathbf{l}$ must be chosen so as to maximize $\mathbf{l}\cdot\boldsymbol{\lambda}$, which, of course, is maximum when $\mathbf{l}$ and $\boldsymbol{\lambda}$ point in the same direction. Thus, $\mathbf{l}$ and $\boldsymbol{\lambda}$ are similarly aligned, and the dot product $\mathbf{l}\cdot\boldsymbol{\lambda}$ is equal to the magnitude of $\boldsymbol{\lambda}$ or λ.

A function L is defined as

$$L = \frac{\lambda}{\mu} - \frac{\lambda_8}{c} \tag{25}$$

and is substituted in Eq. (23) to yield

$$\frac{\alpha_p L}{c} - \frac{\alpha_p^* L^*}{c^*} \geqq 0 \tag{26}$$

In this treatment, c is restricted to be either a continuous variable or a constant, with bounds indicated by Eq. (7). In this case, L is a continuous function, and Eq. (26) reduces to

$$L(\alpha_p - \alpha_p^*) \geqq 0 \tag{27}$$

It will be shown subsequently that α_p is restricted to the values of 1 and 0. It follows from Eq. (27) that

$$L \geqq 0, \alpha_p = 1 \tag{28a}$$

$$L \leqq 0, \alpha_p = 0 \tag{28b}$$

Thus, negative values of L indicate coasting periods along the trajectory. Furthermore, the continuity of K_2 implies that α_p may change in value only at points where L is zero.

Equation (20) implies that either λ_9 is zero (α_p variable) or is zero ($\alpha_p = 1, 0$). If λ_9 is zero, Eq. (19) implies that

$$\lambda_8 = \frac{c\lambda}{\mu} \tag{29}$$

which, when combined with Eqs. (5) and (17), yields

$$\lambda_8 = \frac{\text{constant}}{\mu} \tag{30}$$

However, Eq. (19) then implies that

$$\lambda = \frac{\text{constant}}{c} \tag{31}$$

Now, Eq. (21) shows that λ_{10} is zero in the variable-thrust mode. When λ_{10} is zero, Eq. (18) is incompatible with Eq. (31), from which it follows that Eq. (31) can hold only during the constant-thrust mode, and, therefore,

$$\lambda = \text{constant} \tag{32}$$

The occurrence of a constant λ_8 is extremely unlikely in most potential fields. The two- and three-dimensional harmonic-oscillator potential is a noticeable exception. Lawden (Ref. 7) has recently discussed this singular case for a two-dimensional inverse-square field. Corben (Ref. 8) has shown for this case that the direction of $\boldsymbol{\lambda}$ relative to the local horizontal is constrained to lie within approximately 35 deg of the local horizontal. The combinations of the two constraints of constant λ_8 and bounded direction rule out Eq. (32) for the particular planetary rendezvous and round-trip missions to be discussed. For this treatment, then, it follows that λ_9 is not zero except at discrete points along the trajectory, and, therefore, the thrust parameter α_p is zero or unity, depending upon the sign of L.

Consider the transfer from one thrust mode to the other. If λ_{10} is zero, it follows from Eq. (18) that

$$\frac{\beta}{c^2}\alpha_p\left(L - \frac{\lambda}{2\mu}\right) = 0 \tag{33}$$

and since $\lambda/2\mu$ is positive, the non-trivial conclusion is that L is positive and that, during the variable-thrust mode (VTM),

$$L - \frac{\lambda}{2\mu} = 0 \qquad \text{(VTM)} \tag{34}$$

and the value of α_p is equal to unity. Equations (34), (25), and (17) then yield

$$\lambda_8 = \frac{A}{\mu^2} \qquad \text{(VTM)} \tag{35}$$

which, in turn, yields for the exhaust velocity

$$c = \frac{2A}{\mu\lambda} \qquad \text{(VTM)} \tag{36}$$

and, for the thrust acceleration,

$$a = \frac{\beta\lambda}{2A} \qquad \text{(VTM)} \tag{37}$$

where A is a constant determined by initial conditions. If λ_{10} is not zero, η must be zero, and the constant-thrust mode (CTM) is operative. In this case, L is unrestricted and is given by Eq. (25). In numerical studies, it has been convenient to eliminate λ_8 because of its dependence on exhaust velocity. In the limiting case of infinite exhaust velocity (constant-thrust acceleration), both Eqs. (17) and (25) encounter difficulty. This is obviated by employing a differential equation in L in place of Eq. (17). It is easily shown for the constant-thrust mode, using Eqs. (5), (17), and (25), that

$$\dot{L} - \frac{\dot{\lambda}}{\mu} = 0 \qquad \text{(CTM)} \tag{38}$$

In summary, the continuity of K_2 requires that the transfer from one thrust mode to another occur when the conditions

$$L = \frac{\lambda}{2\mu} \tag{39a}$$

$$\eta = 0 \tag{39b}$$

occur simultaneously. The thrust acceleration in the constant-thrust mode (CTM) is given by

$$\mathbf{a} = \frac{\beta}{c}\,\frac{\alpha_p}{\mu}\,\frac{\boldsymbol{\lambda}}{\lambda} \qquad c = c_{\max} \text{ or } c = c_{\min} \tag{40}$$

and, in the variable-thrust mode, by

$$\mathbf{a} = \frac{\beta\boldsymbol{\lambda}}{2A} \tag{41}$$

A diagram showing the switching sequence just described is shown in Fig. 1 for a 184-day Mars rendezvous trajectory. The variation of the exhaust velocity for this trajectory is shown in Fig. 2.

A typical rendezvous trajectory customarily starts with the exhaust velocity at the lower limit $c_{\min}$. When the conditions become appropriate, a change is made to the variable-thrust mode, during which the exhaust velocity increases until it reaches the upper limit $c_{\max}$. At this point, the vehicle operates at a constant thrust, with an exhaust velocity equal to $c_{\max}$. During this interval, a coast period may or may not be called for; in the example presented in Figs. 1 and 2, a coast period is desired. It is important to note that a coast period on an optimum trajectory is only allowed during the time the vehicle is operating with the exhaust velocity equal to $c_{\max}$. After some time, the conditions will become such that a return to the variable-thrust mode is desired. The trajectory may end in this mode, or, as in the example, a return to the constant-thrust mode, with $c = c_{\min}$, will occur.

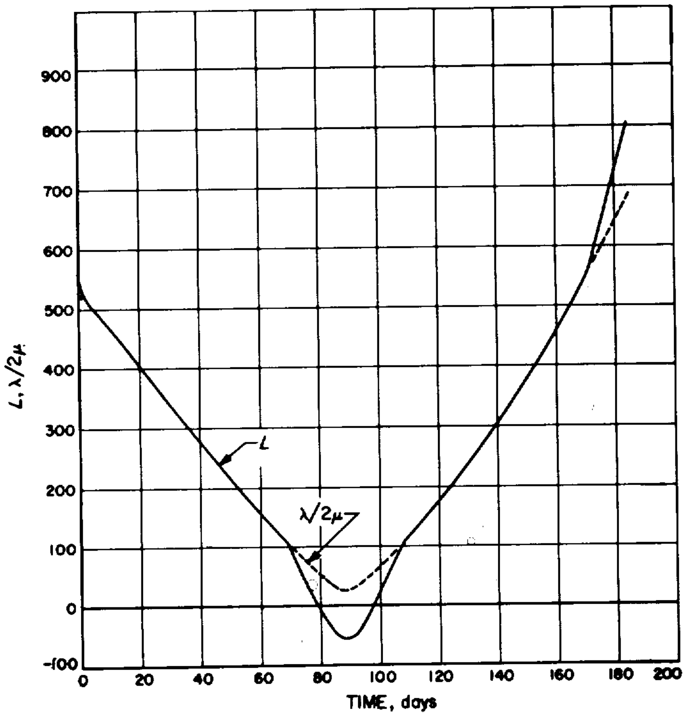

Fig. 1. Thrust-mode transfer sequence, 184-day Mars trajectory

A comparison of the performance of a vehicle using the various thrust options is interesting. Using $\int a^2\,dt$ as a criterion of vehicle performance as described in Section III, the values shown in Table 1 result.

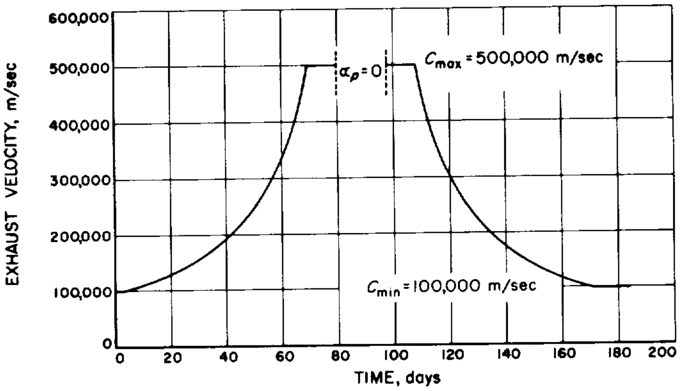

Fig. 2. Exhaust velocity vs time, 184-day Mars trajectory

Table 1. Comparison of vehicle performance

c_{min}, m/sec	c_{max}, m/sec	$\int a^2 dt$ kw/kg $\times 10^3$	Comments
0	∞	6.5760	Variable thrust only
0	500,000	6.5903	Upper limit only
100,000	500,000	6.6196	Both limits
100,000	100,000	7.9493	Constant thrust only
118,500	118,500	7.5520	Optimum constant thrust

III. OPTIMIZATION CRITERIA

Three criteria which may be considered are (1) final vehicle mass, (2) minimum $\int a^2\,dt$, and (3) minimum flight time for a given final vehicle mass. The variable-thrust program optimizes all three of these criteria simultaneously if the exhaust power is constant. The constant-thrust program, however, possesses coast periods, and, by allocating different-length coast periods, one can obtain trajectories satisfying different criteria.

From the calculus of variations, certain transversality conditions hold at the end points of the trajectory. There may be boundary conditions which can be formulated in terms of the variables of the problem. Let these conditions be described by the function

$$A_\nu\left(q_i(t_0), q_i(t_1), t_0, t_1\right) = 0 \qquad \nu = 1, 2, \cdots, \leqq 2n+1 \tag{42}$$

The transversality condition for this Mayer formulation is, thus,

$$\left[dH + \left(K_2\,dt + \frac{\partial F}{\partial \dot{q}_i}\,dq_i\right)\right]_{t=t_0}^{t=t_1} = 0 \tag{43}$$

where

$$H = J + \rho_\nu A_\nu \tag{44}$$

and

$$dH = dJ + \rho_\nu \frac{\partial A_\nu}{\partial q_i}\,dq_i + \rho_\nu \frac{\partial A_\nu}{\partial t} \tag{45}$$

where the ρ_ν are constant multipliers to be determined at the end points and J is the function to be minimized. The dq_i are arbitrary total variations in the variables at the end points subject to the condition that the expressions in Eq. (42) be satisfied. If the value of a variable is specified explicitly at the end point, the corresponding variation is zero.

The optimization is now applied to the criterion of maximum final mass for fixed end conditions. At a fixed terminal time, let the quantity to be minimized be some function of the final mass; namely,

$$J = -k\mu(t_1) \tag{46}$$

where k may be some abitrary positive constant.

Let all the remaining end conditions be independent of μ. An application of Eq. (43) yields

$$\lambda_8(t_0) = \text{unspecified} \tag{47}$$

$$\lambda_8(t_1) = k \tag{48}$$

It is observed, however, that Eqs. (15) to (23) are homogeneous in the Lagrange multipliers; they may, therefore, be scaled without affecting the trajectory, and it follows that Eqs. (47) and (48) are superfluous as boundary conditions. Consequently, it is quite unnecessary to relate a particular Lagrange multiplier to some variable such as μ, as some writers have done. The important point is that for specified values of β and c and for specified terminal conditions, the Euler–Lagrange equations guarantee an extremal in μ by optimum programming of the thrust vector.

However, for a particular β and for specified end conditions, there is an optimum choice of exhaust velocity c which maximizes the final vehicle mass. Isolating this value of c may be accomplished by introducing a new constraining equation into the formulation in the form

$$G_{11} = \frac{\beta}{c^2}\dot{c} = 0 \tag{49}$$

and ignoring Eq. (18), since c is a constant. The Euler–Lagrange equation for the exhaust velocity thus becomes

$$\dot{\lambda}_{11} - \alpha_p\left(2L - \frac{\lambda}{\mu}\right) = 0 \tag{50}$$

and the transversality condition yields

$$\lambda_{11}(t_0) = \lambda_{11}(t_1) = 0 \tag{51}$$

A trajectory which terminates with a value of zero for λ_{11} therefore possesses an extremal in μ with respect to c.[1] The last entry in Table 1 is the optimum c for that mission (Mars rendezvous, launch date 5/13/71, flight time 184 days) and the value of β (0.1 kw/kg) which was used.

Now, consider the minimization of $\int a^2\,dt$. Satisfying Eq. (51) also yields an extremal in this integral with respect to c, since it may be written as

$$\int_{t_0}^{t_1} a^2\,dt = \beta\left[\frac{1}{\mu(t_1)} - \frac{1}{\mu(t_0)}\right] \tag{52}$$

---

[1] Implicit in this process and also in the variable-thrust program is the assumption that β is independent of c. In an actual propulsion system, β is related to c through the efficiency of conversion of power from the power plant to the rocket exhaust power. The quantity λ_{11} may be modified to include the variation of efficiency with c and generally leads to somewhat higher values of c. This will be discussed more fully in a subsequent report.

It is advantageous, however, to consider the minimization of this integral for a fixed c and fixed t_1 by changing the initial thrust acceleration a_0. This integral is fairly insensitive to the value chosen for c, so long as it is in the range typical of low-thrust propulsion systems; it approaches a limiting value for infinite exhaust velocity. Dividing by c to deal also with the limiting case, an a_0 will be found which extremizes the expression

$$\frac{1}{c}\int_{t_0}^{t_1} a^2\,dt = a_0\left[\frac{1}{\mu(t_1)} - \frac{1}{\mu(t_0)}\right] \qquad \mu(t_0) = 1 \tag{53}$$

The approach is the same as that followed in Eq. (49); the additional constraining relation

$$G_{12} = \dot{a}_0 = 0 \tag{54}$$

is introduced, with Eq. (18) again being ignored. The resulting Euler–Lagrange equation is

$$\dot{\lambda}_{12} + \alpha_p L = 0 \tag{55}$$

An application of Eq. (43) yields

$$\lambda_{12}(t_0) = 0 \tag{56}$$

At the terminal point, both a_0 and $\mu = \mu(t_1)$ are unspecified. Thus, upon minimizing the function,

$$J = \frac{k}{c}\int_{t_0}^{t_1} a^2\,dt = ka_0\left(\frac{1}{\mu} - 1\right) \tag{57}$$

of the endpoints, where k is again some arbitrary constant, Eq. (43) will yield the following two equations:

$$\lambda_8 - \frac{ka_0}{\mu^2} = 0 \tag{58}$$

$$\lambda_{12} + k\left(\frac{1}{\mu} - 1\right) = 0 \tag{59}$$

which, upon eliminating k, yields the transversality condition

$$\left[\lambda_{12} + \mu(1-\mu)\frac{\lambda_8}{a_0}\right]_{t_1} = 0 \tag{60}$$

to be satisfied at the terminal point so that J in Eq. (57) will be an extremal with respect to a_0. This transversality condition, upon applying Eqs. (5), (17), and (25), becomes

$$\Big[\mu(\lambda - \mu L)\Big]_{t_0}^{t_1} = 0 \tag{61}$$

For minimum-time trajectories with specified end conditions and specified final mass $\mu(t_1)$ or $\int a^2\,dt$, the propulsion system is simply forced to operate over the entire trajectory.

IV. INTERPLANETARY RENDEZVOUS TRAJECTORIES

In a planetary rendezvous mission, six terminal quantities must be specified; it is convenient to group these into five which determine the size and orientation of the terminal orbit and one quantity which determines the rendezvous point on the orbit. These first five quantities are the semimajor axis and eccentricity or, equivalently, the energy and angular momentum of the terminal ellipse, and the orbital inclination, the argument of perigee, and the longitude of the line of the ascending node. The position on the ellipse is determined by the true anomaly; that is, the angle from perigee to the rendezvous point.

The optimum orbital transfer or rendezvous occurs when the terminal position on the orbit is left unspecified and the resulting transversality condition derived from Eq. (43) is satisfied. The satisfaction of the transversality condition guarantees an extremal in the quantity being minimized; and both relative maxima and minima may result from satisfying this condition. When the terminal position or rendezvous point is left unspecified, an application of the transversality condition yields

$$\dot{\boldsymbol{\lambda}} \cdot \mathbf{v} + \boldsymbol{\lambda} \cdot \nabla U = 0 \qquad (62)$$

to be satisfied for an extremal in the quantity being optimized with respect to true anomaly.

As an example of the application of this theory to mission feasibility studies, the results from an extensive set of rendezvous trajectories from Earth to Mars and from the Earth to Venus are presented. The formulation of these equations has been programmed on the JPL IBM 7090 digital computer. In order to overcome the two-point boundary-value problem, this program has been coupled with an iterative routine to converge upon the specified terminal conditions. By this procedure, parametric analyses have been conducted efficiently through the large-scale production of interplanetary trajectories with wide ranges of mission conditions and flight times. A description of the present method of solution of the two-point boundary-value problem as applied to the basic trajectory program has been included in the Appendix.

In the first example to be presented, a two-dimensional heliocentric inverse-square central-force-field model is employed. The departing orbit of the Earth is assumed circular, with a radius of one astronomical unit from the Sun. The arrival orbit has the semimajor axis and eccentricity of either the Martian or Venusian orbit, as the case may be. The assumed values for these orbits are:

	Mars	*Venus*
Semimajor axis, AU	1.523691	0.723332
Eccentricity	0.093371	0.0

The terminal conditions are, therefore, specified values of energy and angular momentum; the transversality condition (62) is specified, and in all trajectories, the rendezvous point and the orientation of the terminal orbit are unspecified. By using a polar formulation (Ref. 11) for the equations of motion, a constant of integration K_1 in the Euler equations results from the cyclic nature of the polar angle. It may be shown (Ref. 11) that if the terminal orientation of the orbit is unspecified, the value of K_1 is zero for the fourth condition to be satisfied. Both the variable- and the constant-thrust programs have been used; unless otherwise noted, the exhaust velocity employed in the constant-thrust program is 50 km/sec.

The three trajectory types being considered—(1) variable thrust, (2) constant thrust with an optimum coast period, and (3) constant thrust, minimum time with no coasting period—have been run for flight times ranging from 40 to more than 300 days. The coast period for (2) has been optimized, so that $\int a^2\,dt$ is a minimum, the transversality condition (61) being satisfied. Figure 3 shows the variations of $\int a^2\,dt$ with flight time for rendezvous at both the optimum and the worst point on the Martian orbit. Figure 4 is the equivalent plot of $\int a^2\,dt$ with flight time for an optimum rendezvous on the Venusian orbit, only one set of curves resulting because of the circular end conditions. These Figures afford an interesting comparison between the variable-thrust and the constant-thrust programs. The increase in $\int a^2\,dt$ from using a constant-thrust program with optimum coast instead of a variable-thrust program is about 15%. In typical missions, this produces about a 4% decrease in final vehicle mass, as may be verified directly from Eq. (52). For continuous-thrust interplanetary trajectories, it is known (Refs. 2, 9) that the effect of the planetary orbital inclinations on the value of $\int a^2\,dt$ or final vehicle mass is quite small; in the case of Mars, the 1.85-deg orbital inclination increases the value of $\int a^2\,dt$ in the three-dimensional variable-thrust trajectories by less than 1%. Consequently, Figs. 3 and 4 yield a highly valid estimate of the payload capabilities of power-limited propulsion systems for Mars and Venus rendezvous missions.

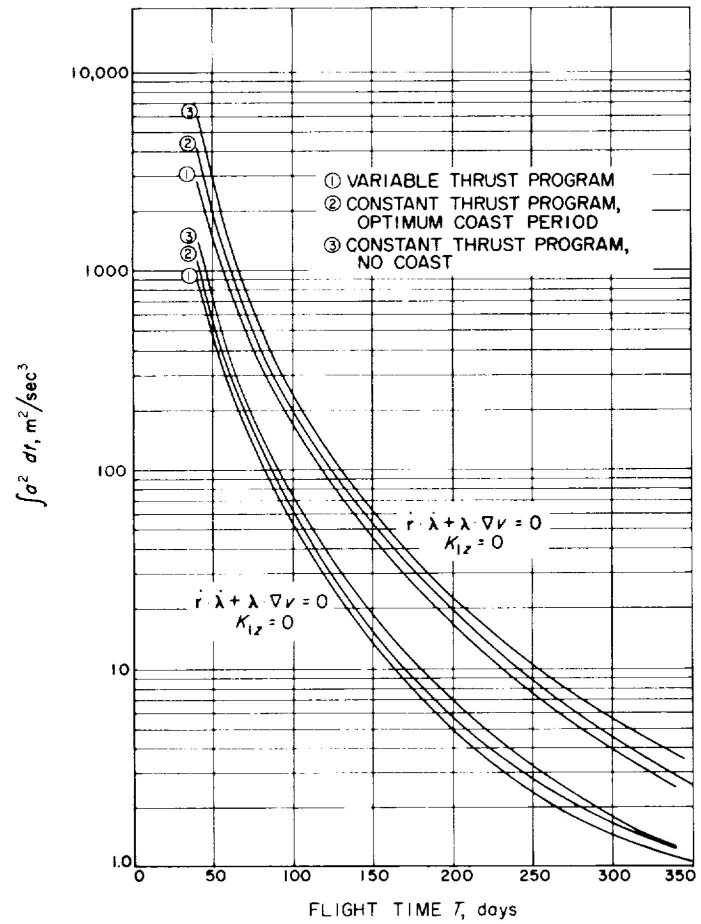

Fig. 3. $\int a^2 dt$ vs flight time, Martian rendezvous trajectories

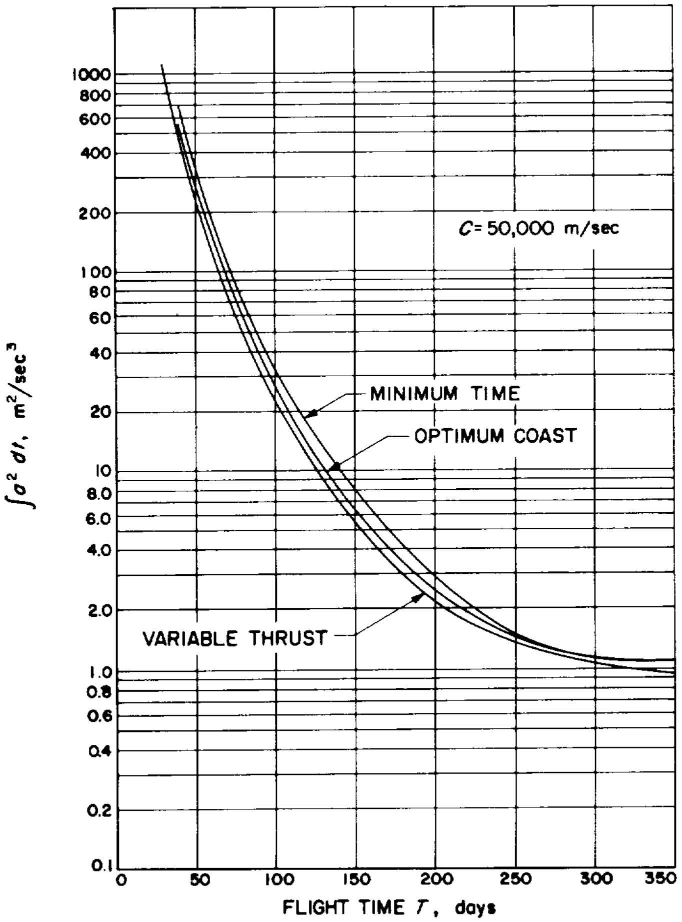

Fig. 4. $\int a^2 dt$ vs flight time, Venusian rendezvous trajectories

The $\int a^2 dt$ is fairly insensitive to the exhaust velocity employed in typical cases, but it does become sensitive for extremely low values or short flight times. Table 2 compares this integral for exhaust velocities of 50,000 m/sec and infinity (constant acceleration) for the Mars optimum coast trajectories.

If payload maximization is the desired end, the procedure which optimizes the value of the exhaust velocity is strictly the proper approach; however, the payload is then strongly dependent upon the value of β employed, and, consequently, this procedure is dependent on the power and efficiency ratings of the particular propulsion system and power supply under consideration. For parametric studies, the $\int a^2 dt$, because of its near invariance to the propulsion-system ratings, is of more utility. A specific example may be found in Ref. 11 for an optimization of the final mass with respect to exhaust velocity.

Table 2. Comparison of $\int a^2 dt$ for exhaust velocities of 50,000 m/sec and ∞

T days	$\int a^2 dt$, kw/kg $\times 10^3$	
	$c = 50{,}000$ m/sec	$c = \infty$
50	556.03	525.11
100	59.821	59.250
150	15.263	15.225
200	5.6225	5.6138
250	2.7279	2.7222
300	1.1380	1.1338

V. THREE-DIMENSIONAL RENDEZVOUS TRAJECTORIES

As a second example, the results from a series of three-dimensional rendezvous trajectories from Earth to Mars are presented. These trajectories utilize the actual positions and velocities of the Earth and Mars during the era of 1970–71 as initial and terminal conditions. A six-dimensional version of the iterative routine was used to obtain these converged trajectories using the variable-thrust program. Figure 5 shows the variation of $\int a^2\,dt$ with heliocentric launch date for three flight times—120, 184, and 360 days. The minima of these curves correspond to a planetary configuration in which the transversality condition that Eq. (62) have the same initial and terminal value (not necessarily zero) is satisfied.

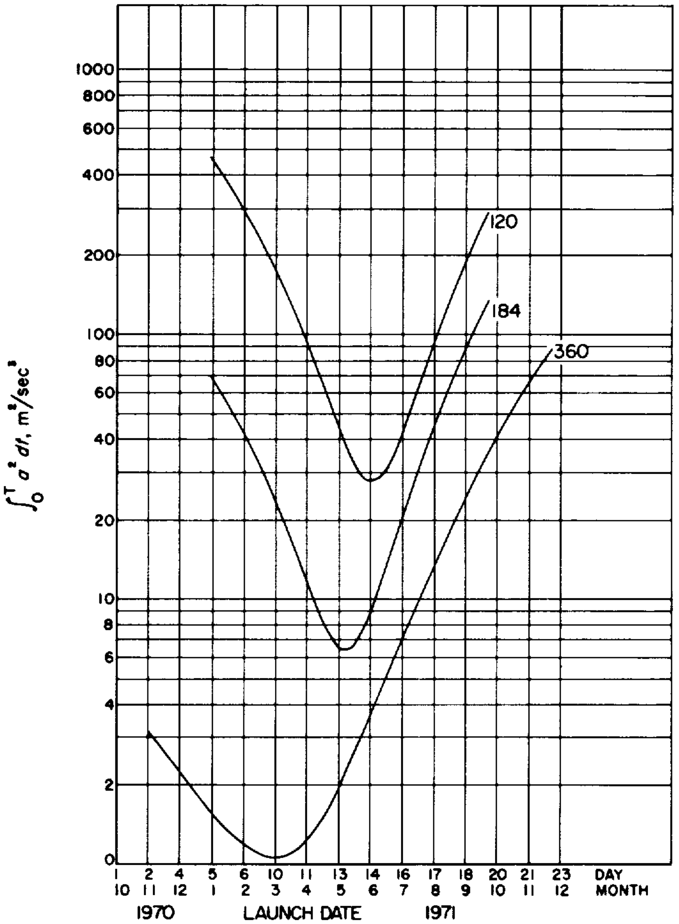

Fig. 5. $\int a^2 dt$ vs launch date; 120-, 184-, and 360-day Martian rendezvous trajectories during 1970–71

The year 1971 is a "vintage year" for low-thrust trajectories to Mars, because both the transversality condition (62) and a zero value of K_1 are nearly simultaneously satisfied for all flight times, and the trajectories rendezvous very close to the optimum point on the Martian orbit. Thus, the minima of these curves fall almost exactly along the lower variable-thrust curve in Fig. 3. For the subsequent synodic era in 1973, the minima have a larger value of $\int a^2\,dt$, and by 1977 and 1979, the Earth–Mars configuration is such that the trajectories rendezvous near the least-optimum point and the minima, occurring late in these years, lie near the upper variable-thrust curve in Fig. 3. In any era, the minima are bounded between these two curves in Fig. 3. Figure 6 exhibits contours of equal $\int a^2\,dt$ with flight time versus heliocentric launch date. From these Figures, the range of optimum launch dates for either minimum $\int a^2\,dt$ or minimum flight time may be found. The locus of minimum flight time for a given $\int a^2\,dt$ will pass, for zero flight time, through the date of opposition, which is about August 10, 1971.

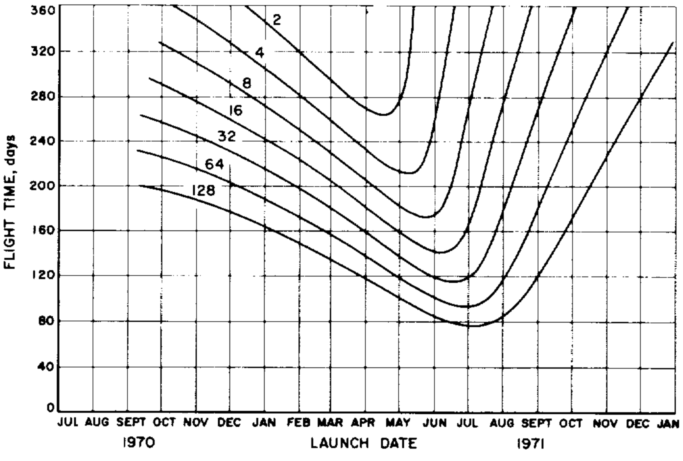

Fig. 6. Contours of equal $\int a^2 dt$, flight time vs launch date for Martian rendezvous trajectories during 1970–71

These curves are not unique, because there exist classes of trajectories yielding extremals in $\int a^2\,dt$ which, for a given launch date and flight time, rendezvous Mars but make an arbitrary number of circuits around the Sun either in the forward or retrograde directions. Of particular interest is that class of trajectories which make one additional circuit around the Sun and which correspond to the optimum set in the following synodic era of 1973, just as the ones shown are optimum for the 1970–71 era. For a given flight time, there clearly exists a launch date which is a trade-off point and for which, for later dates, the optimum path is obtained by adding to the transit required to rendezvous Mars.

The increased steepness on the ascending branches of these curves may be explained in terms of the decreasing transit angle of the trajectory with increasing launch dates as the Earth and Mars approach opposition. A more radical thrust program than that for the minimum transfer is required to accomplish the mission.

The shape of these curves is nearly the same when a constant-thrust program is employed. The minima occur at almost precisely the same dates, within one or two days. The values of $\int a^2\,dt$, as explained in Section IV, will increase by approximately 15%.

VI. INTERPLANETARY ROUND-TRIP TRAJECTORIES

Considerable simplification is possible in making preliminary round-trip calculations for transfer between the Earth and the other planets by assuming that the orbits of the Earth and the destination planet are coplanar and circular. A round-trip mission can generally be divided into the following phases: (1) an Earth escape, (2) an Earth–planet transfer, (3) planetocentric capture, (4) a waiting or reconnaissance time at the planet, (5) planetocentric escape, (6) a planet–Earth transfer, and (7) an Earth capture. In many instances, only a loosely bound orbit may be required at the destination planet, so that the propellant requirements for phases (3) and (5) may be negligible. If a relatively tightly bound orbit is required, however, the propellant consumption would need to be considered for these phases.

In the following analysis, the emphasis is solely upon the heliocentric phases of the trajectory; propellant requirements may be made for the Earth-escape and -capture phases and the planet-capture and -escape phases by referring to Ref. 9. A further simplification is possible by utilizing a variable-thrust program for the heliocentric-transfer phases, the $\int a^2\,dt$ derived for the variable-thrust program being approximately 15% less than for the equivalent mission utilizing a constant-thrust program with an optimum coast period.

VII. ROUND-TRIP TRAJECTORY CALCULATIONS FOR AN EARTH-TO-MARS MISSION

Let T_{F1} be the flight time in days and θ_{T1} the transit angle covered during this time for the Earth-to-Mars phase, and let T_{F2} and θ_{T2} be the equivalent quantities for the Mars-to-Earth phase. If the launch time, reckoned from opposition, is denoted by T_{L1}, then, for the Earth-to-Mars phase,

$$(n_e - n_m) T_{L1} = n_m T_{F1} - \theta_{T1} \qquad (63)$$

and for the Mars-to-Earth phase,

$$(n_e - n_m) T_{L2} = \theta_{T2} - n_e T_{L2} \qquad (64)$$

where n_e and n_m are the mean daily motion of the Earth and Mars, respectively. Values of the mean daily motion of these two planets may be had from the *American Ephemeris and Nautical Almanac* and are

$$n_e = 0.985647 \text{ deg/day}$$

$$n_m = 0.524033 \text{ deg/day}$$

In the case of orbital transfer or rendezvous, the maximum payload results when the transversality condition (62) is satisfied. For the variable-thrust program, the optimum transit angle which results when (62) is satisfied may be approximated quite accurately as a function of flight time T_F in days by

$$\theta_T(\text{optimum}) = 4.298 + 0.706\, T_F \text{ deg} \qquad (65)$$

for coplanar transfer between circular orbits of the Earth and Mars or between Mars and the Earth. Using the optimum value of θ_T in Eqs. (63) and (64), the optimum launch times for Earth to Mars and for Mars to Earth may be determined. Thus,

$$T_{L1}(\text{optimum}) = -9.311 - 0.394\, T_{F1} \qquad (66)$$

$$T_{L2}(\text{optimum}) = 9.311 - 0.606\, T_{F2} \qquad (67)$$

Now, the arrival time at Mars is found by adding T_{F1} to T_{L1}:

$$T_{A1}(\text{optimum}) = -9.311 + 0.606\, T_{F1} \qquad (68)$$

A cursory examination of T_{A1} and T_{L2} in Eqs. (67) and (68) above reveals the interesting fact that it is not possible to launch on the optimum date for both outgoing and incoming phases of the trajectory unless one waits nearly a full synodic period of Mars ($T_{\text{synodic}} = 779.94$ days) before returning to the Earth. If a shorter total trip time is desired, a compromise must be made on one or both phases of the trajectory by intercepting one or the other planet at a non-optimum point on the orbit.

As an example of a typical mission, a number of Earth–Mars round-trip trajectories were calculated, in which the total heliocentric trip time was 544 days, including 496 days under power and a 48-day waiting period at Mars. The results of this investigation are shown in Fig. 7, which is a graph of $\int a^2\,dt$ versus launch time for several combinations of powered flight times which satisfied the relation $T_{F1} + T_{F2} = 496$ days.

Contrary to what may have been expected, the minimum values of $\int a^2\,dt$ for this particular example do not occur when the total powered flight time is divided equally between T_{F1} and T_{F2} but rather somewhere near the ratio of $5T_{F1}{:}3T_{F2}$. Thus, curve 3 in Fig. 7 for $T_{F1} = 184$ days and $T_{F2} = 312$ days presents the minimum value of the integral. Furthermore, the minimum value

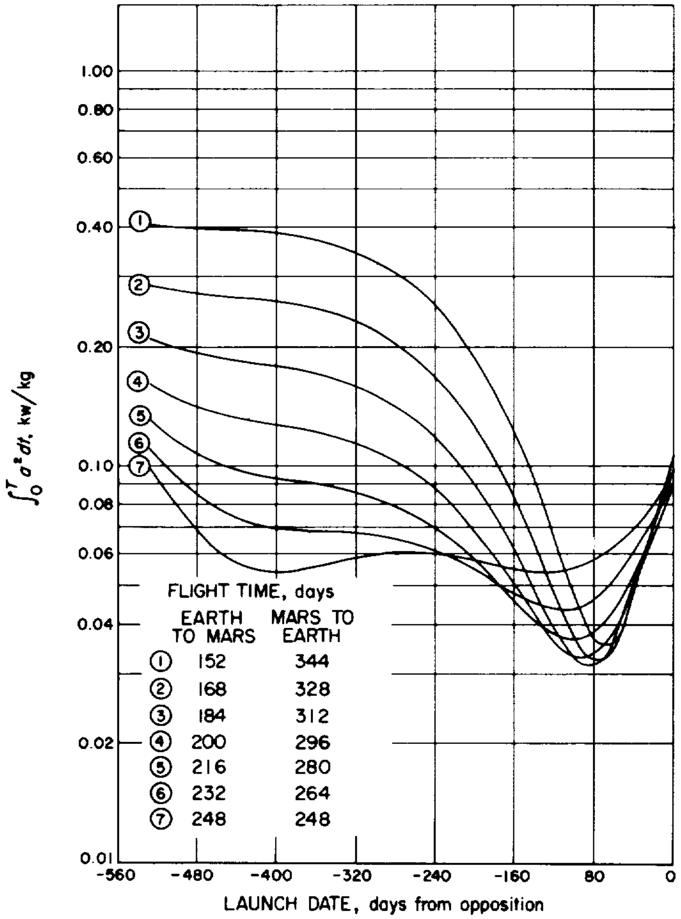

Fig. 7. $\int a^2 dt$ vs launch date, 544-day Martian round trip with circular end conditions

of the integral occurs at a launch time which very nearly corresponds to the optimum launch time for the shorter flight time; in this case, T_{F1}.

It is important to note at this point that the combination of $T_{F1} = 312$ days and $T_{F2} = 184$ days is equally acceptable, this combination not being shown in Fig. 7, since it is the mirror image of $T_{F1} = 184$ days and $T_{F2} = 312$ days. The optimum launch time is such that the shorter flight time occurs nearly optimally. The optimum Earth-to-Mars launch time occurs, for this latter case, at $T_{L1} = -488$ days, as contrasted to $T_{L1} = -80$ days for the example used in Fig. 7.

The effect of increasing or decreasing the waiting time at Mars while keeping the powered flight time fixed is to increase or decrease the value of $\int a^2\,dt$, a 100-day waiting period having the effect of increasing the value of the integral by about 20% over the equivalent trajectory with no waiting period. The effect of shortening the total powered flight time is to increase the value of the integral. Lengthening the powered flight time does the opposite; i.e., it decreases the value of the integral.

The Mars-to-Earth transfer phase with the longer flight time, $T_{F2} = 312$ days, accomplishes rendezvous with the Earth at some distance from the optimum transit angle. For the trajectory, which corresponds to the minimum value of $\int a^2\,dt$ in Fig. 7, the transit angle is about 135 deg greater than optimum. It is characteristic of the transfer trajectories between circular coplanar orbits, where the transit angle is greater than optimum, that the transfer orbit will pass within the orbit of the Earth; in the present example, the path comes to within approximately 0.5 AU of the Sun. These optimum trajectories are quite similar in some respects to the non-optimum transfer trajectories employed by W. E. Moeckel of the Lewis Research Center (Ref. 10).

VIII. A THREE-DIMENSIONAL EXAMPLE OF A 1971–1972 MARS ROUND-TRIP MISSION

In order to present a more sophisticated example of a Mars round-trip mission, a three-dimensional analysis was conducted for an era 1971–72, in which the actual ephemeris positions of the two planets were matched at the appropriate rendezvous points. The example presented here is that which matched as closely as possible the conditions of the trajectory which produced the minimum value of $\int a^2\,dt$ in Fig. 7.

The following heliocentric launch and arrival dates were found appropriate for this example:

Launch date, Earth-to-Mars transfer, May 13, 1971

Arrival date at Mars, November 11, 1971

Launch date, Mars-to-Earth transfer, December 31, 1971

Arrival date at the Earth, November 7, 1972

As before, the flight times are $T_{F1} = 184$ days and $T_{F2} = 312$ days.

In order to calculate the exhaust velocity required and the propellant consumption, a value of 5 kg/kw was assumed for the specific weight α of the power plant, this value being typical of those being used in other vehicle studies (Ref. 10). In addition, a power-plant-weight to initial-weight ratio of 0.25 was assumed. The resulting value of the quantity β used in the variational formulation is thus 0.1 kw/kg.

Plots of the projection of the trajectory on the ecliptic plane are shown in Figs. 8 and 9. The Earth-to-Mars transfer shown in Fig. 8 has a transit angle of 145 deg and a value of $\int a^2\,dt$ of 0.006576 kw/kg. The behavior of the return trip shown in Fig. 9 is as described previously: the trajectory passes within the orbit of the Earth at around 126 days and thus spends about 186 days within the orbit of the Earth on the return voyage. The transit angle for the return voyage is almost exactly 360 deg and the value of $\int a^2\,dt$ is 0.024990 kw/kg.

The manner in which the exhaust velocity varies during the trip is shown in Fig. 10. As may be seen in Table 1, it is most likely that the total excursion of the exhaust velocity could be reduced considerably by introducing maximum and minimum constraints of the exhaust velocity of $c_{\min} \leq c \leq c_{\max}$ without adversely affecting the value of the $\int a^2 dt$.

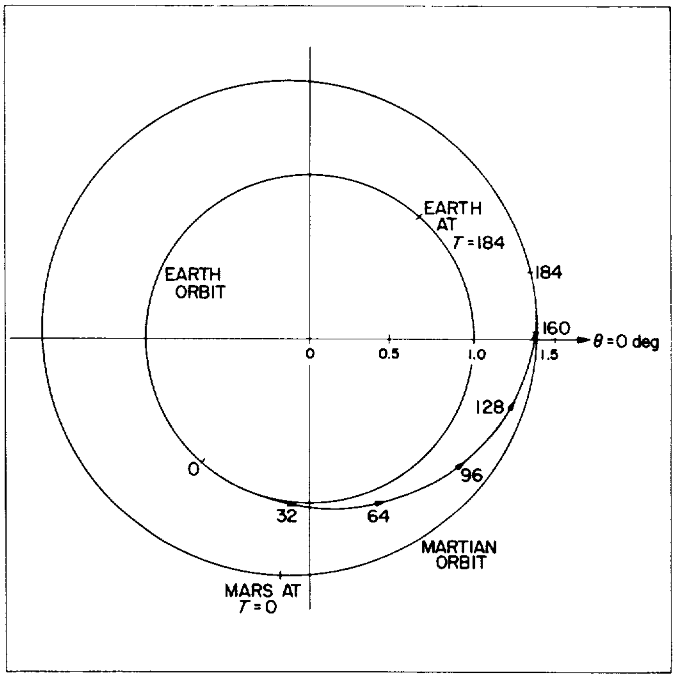

Fig. 8. Earth-to-Mars transfer trajectory, 184-day flight time, ecliptic projection

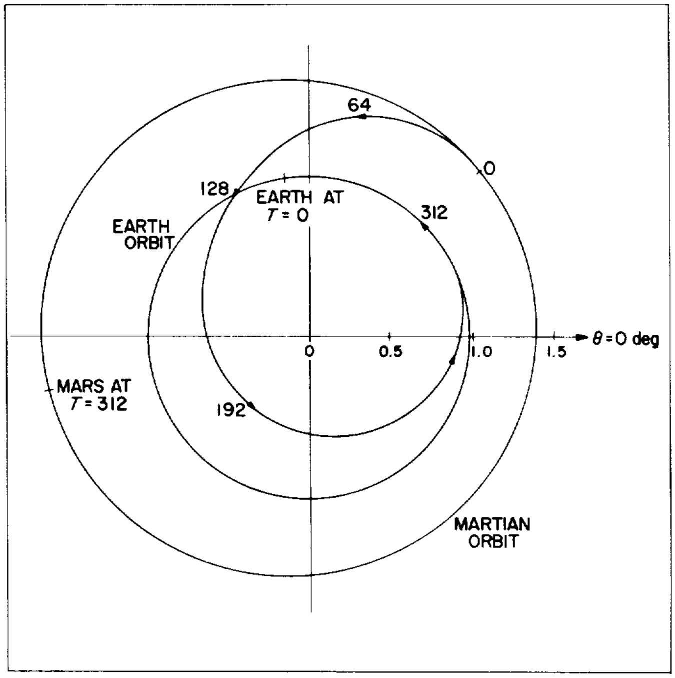

Fig. 9. Mars-to-Earth transfer trajectory, 312-day flight time, ecliptic projection

The total fractional mass remaining at the end of the voyage (for the heliocentric phase only) is given by

$$\frac{M_{\text{initial}}}{M_{\text{final}}} = 1 + \frac{1}{\beta}\left(\int_0^{T_{F1}} a^2\,dt + \int_0^{T_{F2}} a^2\,dt\right) \tag{69}$$

and, using the values of the appropriate quantities,

$$\frac{M_{\text{initial}}}{M_{\text{final}}} = 1 + \frac{1}{0.1}(0.006576 + 0.024990) \tag{70}$$

yields

$$\frac{M_{\text{final}}}{M_{\text{initial}}} = 0.760 \tag{71}$$

Since the power-plant weight ratio was assumed to be 0.25, the useful payload is 0.51 of the initial weight injected into the heliocentric phase. The manner in which the mass ratio varies as a function of trip time is shown in Fig. 11.

A comparison of the $\int a^2\,dt$ between the three-dimensional example just presented and the example using coplanar, circular end conditions which produced the minimum $\int a^2\,dt$ in Fig. 7 is interesting (see Table 3).

Table 3. Comparison of $\int a^2 dt$ for three-dimensional example and example using coplanar, circular end conditions

Phase	$\int a^2 dt$	kw/kg
	Three-dimensional	Circular, coplanar
Earth to Mars	0.006576	0.012909
Mars to Earth	0.024990	0.019019
Total	0.031566	0.031928

Apparently, the conditions for the three-dimensional example are such that, although, as expected, the Earth-to-Mars phase produces a lower value for $\int a^2\,dt$ than for circular conditions, the effects of the eccentricity of the Martian orbit on the Mars-to-Earth phase result in a larger value for $\int a^2\,dt$ than for the equivalent mission using circular end conditions. The net result is that the total $\int a^2\,dt$ appears approximately the same for the exact three-dimensional example and for the example

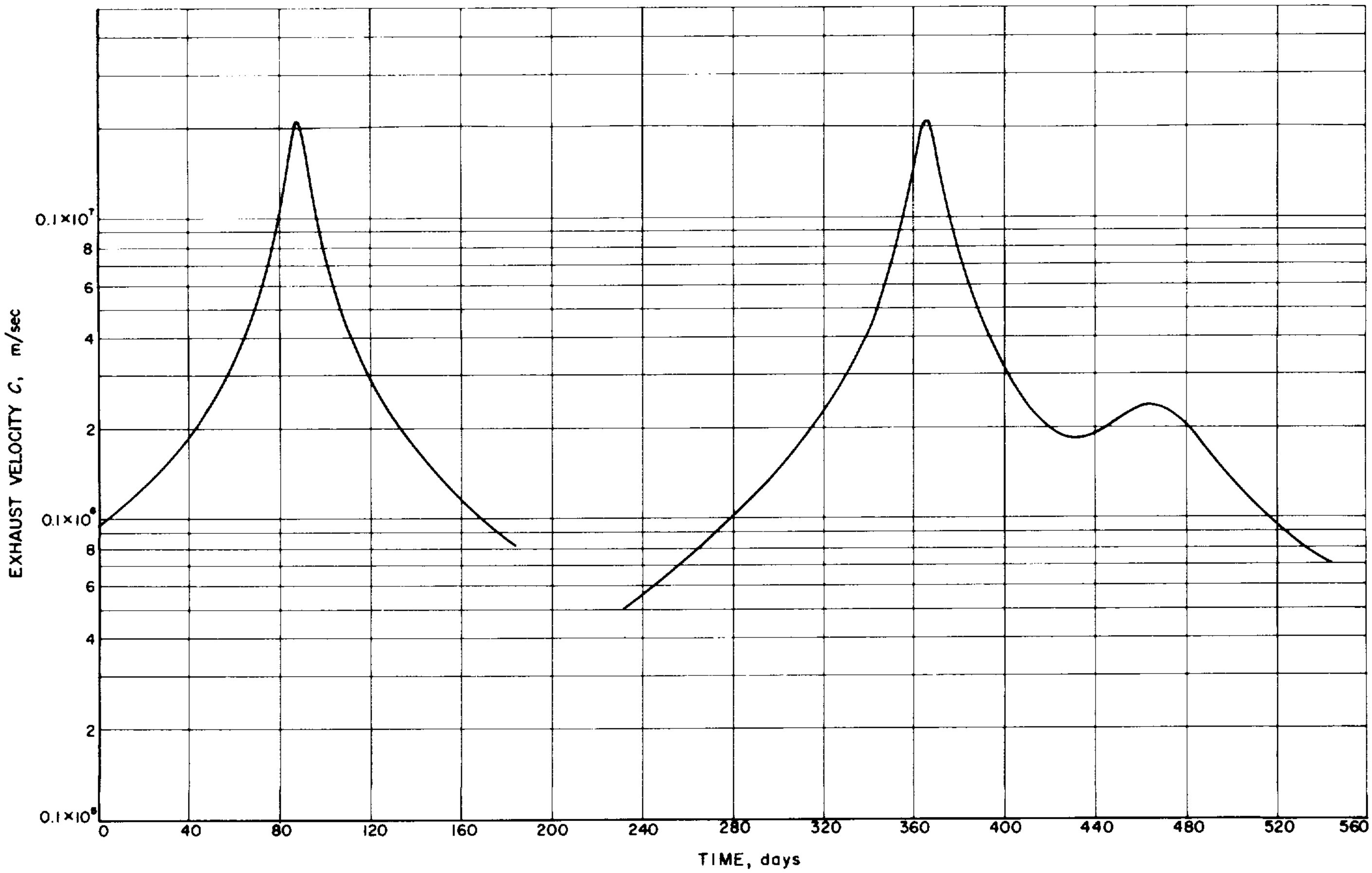

Fig. 10. Exhaust velocity vs time, 544-day Martian round trip

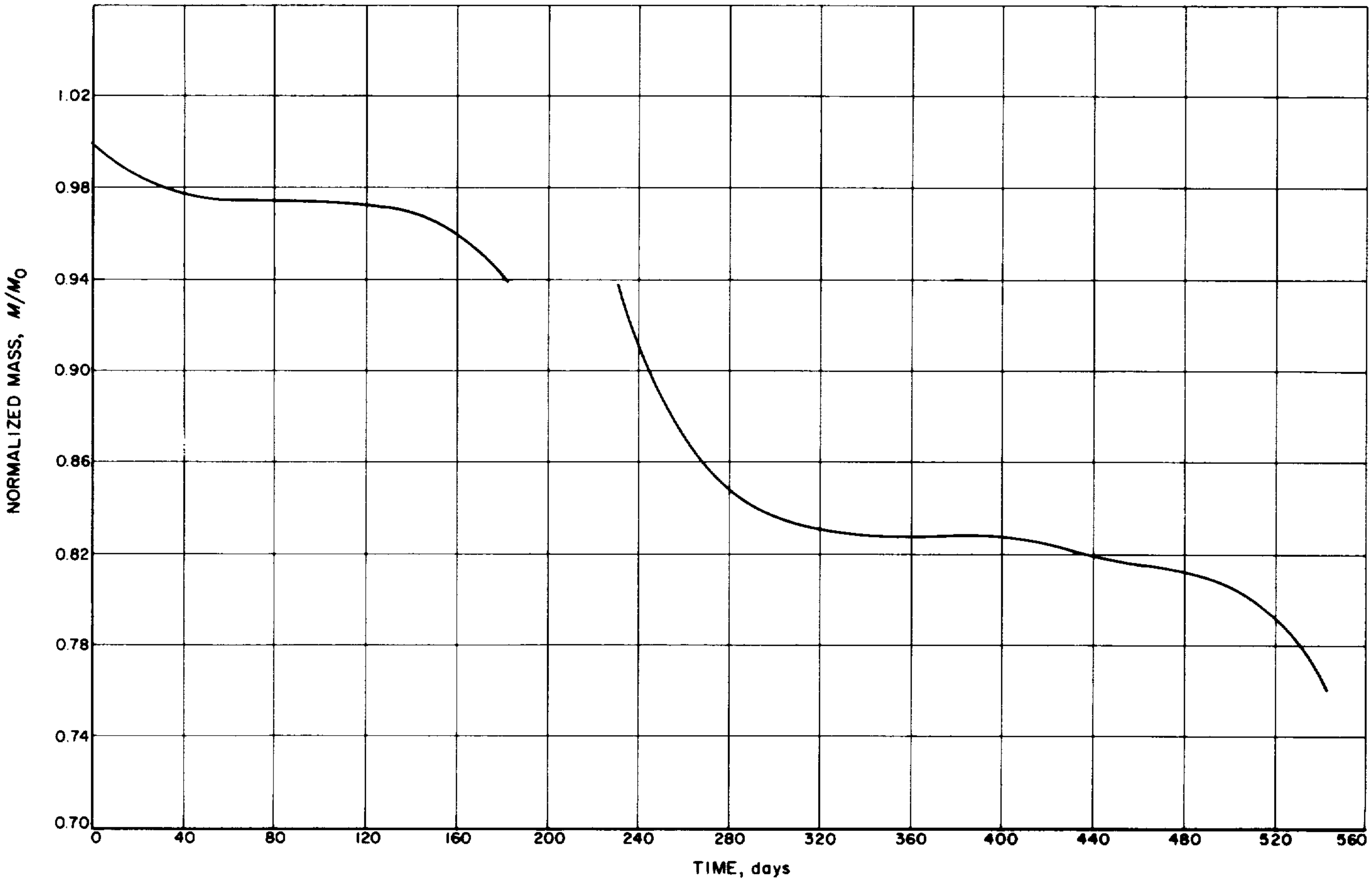

Fig. 11. Normalized vehicle mass vs time, 544-day Martian round trip

with circular, coplanar end conditions. Whether this is true in general remains to be determined.

Although the use of coplanar, circular end conditions gives a fairly good insight into the payload capabilities, nevertheless the effects of the eccentricity of the Martian orbit on the shape of the curves shown in Fig. 7 should be examined more thoroughly. The effect of the inclination of the Martian orbit on the payload capability has been examined previously for rendezvous trajectories and has the effect of increasing the value of the $\int a^2 \, dt$ slightly. Of more immediate interest, perhaps, would be the influence of various thrust programs on $\int a^2 \, dt$ for these round-trip missions.

REFERENCES

1. Irving, J. H., *Space Technology,* ed. H. S. Seifert, Wiley and Sons, New York, 1959, Chap. 10.
2. Melbourne, W. G., "Three-Dimensional Optimum Thrust Trajectories for Power Limited Propulsion Systems," *ARS Journal,* Vol. 31, No. 12, December 1961, p. 1723.
3. Bliss, G. A., *Lectures on the Calculus of Variations,* The University of Chicago Press, Chicago 1946, Chap. 7.
4. Miele, A., "An Extension of the Theory of the Optimum Burning Program for the Level Flight of a Rocket-Powered Aircraft," *J. Aeronautical Sciences,* Vol. 24, 1957, p. 874.
5. Lawden, D. F., *Advances in Space Science,* ed. F. I. Ordway III, Academic Press, New York, 1959, Vol. 1, Chap. 1.
6. Leitmann, G., "On a Class of Variational Problems in Rocket Flight," *J. Aero-Space Sciences,* Vol. 26, 1959, p. 586.
7. Lawden, D. F., "Inter-Orbital Transfer of a Rocket," *J. British Interplanetary Soc.,* Annual Report, 1952, p. 321.
8. Corben, H. C., *A Note on the Optimization of Powered Trajectories,* ERL-LM-150, Ramo Wooldridge Corporation, December 4, 1957.
9. Melbourne, W. G., *Interplanetary Trajectories and Payload Capabilities of Advanced Propulsion Vehicles,* Technical Report No. 32-68, Jet Propulsion Laboratory, Pasadena, Calif., 1961.
10. Moeckel, W. E., *Fast Interplanetary Missions with Low-Thrust Propulsion Systems,* NASA Technical Report R-79, Lewis Research Center, Cleveland, Ohio, 1960.
11. Melbourne, W. G., and Sauer, C. G., Jr., *Optimum Thrust Programs for Power-Limited Propulsion Systems,* Technical Report No. 32-118, Jet Propulsion Laboratory, Pasadena, Calif., 1961 (also ARS Preprint 2075-61).

APPENDIX

I. SEARCH PROCEDURE FOR LOW-THRUST POWER-LIMITED PROPULSION SYSTEMS

A standard Newton–Raphson method is employed, where a partial matrix is calculated numerically by perturbing x_i. The problem solved is of the form

$$|F_i(x_i \cdots x_N) - Y_i| \leq e_i \qquad i = 1 \cdots N$$

where F_i may be a nonlinear function of x_i. (The desired values of the F_i are the Y_i. The degree of convergence required between Y_i and F_i is e_i.)

The partial matrix is formed by computing a standard or nominal set of values $F(x_i)_s$ and a set of perturbed values $F(x_i)_p$ by perturbing the nominal x_i from $i = 1 \cdots N$. This is accomplished by integrating the given set of differential equations as a function of time using a Runge–Kutta fourth-order numerical integration scheme as a starting integrator until n differences are obtained for integrating with an Adams–Moulton predictor–corrector integration package. Presently, $n = 5$. The augmented partial matrix stored is of the form

$$\begin{bmatrix} \dfrac{F_1 - F_{1s}}{x_1 - x_{1s}} & \cdots & \dfrac{F_N - F_{Ns}}{x_1 - x_{1s}} \\ \cdot & & \cdot \\ \cdot & & \cdot \\ \cdot & & \cdot \\ \dfrac{F_1 - F_{1s}}{x_N - x_{Ns}} & \cdots & \dfrac{F_N - F_{Ns}}{x_N - x_{Ns}} \end{bmatrix} \begin{bmatrix} \Delta Y_1 \\ \cdot \\ \cdot \\ \cdot \\ \Delta Y_N \end{bmatrix} ;\Delta Y_i = Y_i - F_i \quad i = 1 \cdots N \tag{A-1}$$

where the subscript s represents the standard or nominal values and $i, j = 1, \cdots N$ the perturbed values. The search matrix is

$$A = [a_{ij}] = \left[\frac{F_j - F_{js}}{x_i - x_{is}}\right] \simeq \left[\frac{\partial F_j}{\partial x_i}\right] \qquad i, j = 1 \cdots N \tag{A-2}$$

A Gauss elimination method is then used to solve the system of simultaneous equations thus generated. A set of Δx_i is obtained which are to be added to the nominal x_i to give a new set of nominal $x_i = x_i + \Delta x_i$. An iterative process is thus derived which is concluded either by satisfying the e_i convergence requirement or the conclusion of a specified number of iterations.

However, it is not always desirable from the standpoint of machine time consumed to have to recompute the partial matrix as the above description implies, since this necessitates running a standard trajectory and N perturbed trajectories. To circumvent this, and assuming that the elements of the partial matrices are near linear, an attempt is made to integrate up to five additional nominal trajectories before a recomputation of the partial matrix is executed. If convergence is not obtained within the one to five trajectories, the x_i of the last converging trajectory are used as the nominal x_i for starting the recomputation of the matrix. A loop is then defined to be the sequence starting with a nominal x_i and terminating at one of the one to five trajectories before a recomputation of the partial matrix is deemed necessary. An iteration is defined to be the number associated with each standard or nominal trajectory computed, excluding the first. A slight ambiguity thus arises between the standard trajectory computed after the partial matrix and the first of the one to five trajectories. Let Z represent a trajectory; a typical sequence of computations is:

1 iteration 5 iterations

$$\underbrace{Z_{s0}\,Z_{1p} \cdots Z_{Np}\,\overset{\swarrow}{Z_{s1}}\,\overset{\searrow}{Z_s^1}\,Z_s^2\,Z_s^3\,Z_s^4\,\overset{\downarrow}{Z_s^5}}_{\text{1 loop}}$$

1 iteration 5 iterations

$$\underbrace{Z_{1p} \cdots Z_{Np}\,\overset{\swarrow}{Z_{s2}}\,\overset{\searrow}{Z_s^1}\,Z_s^2\,Z_s^3\,Z_s^4\,\overset{\downarrow}{Z_s^5}\,\cdots}_{\text{2 loops}}$$

It remains to describe the method of perturbing the x_i, which involves adding a δx_{ip} to the x_i for each ith perturbed trajectory. This is accomplished by taking a percentage of the nominal x_i. Thus,

$$x_{ip} = x_{is} + P_i x_{is} \tag{A-3}$$

where P_i = percentage, $i = 1 \cdots N$.

A flow diagram for the preceding search procedure is shown in Fig. A-1.

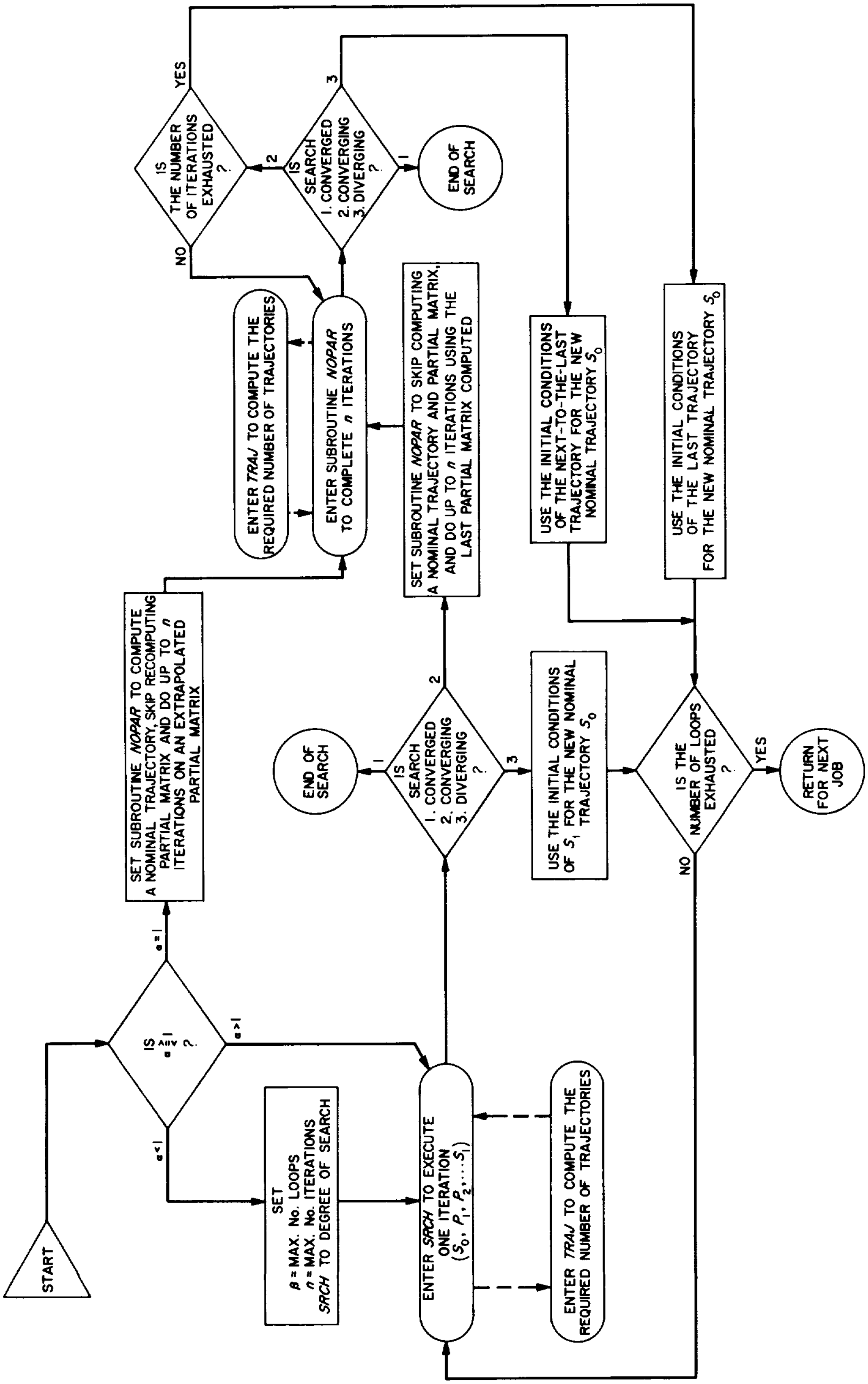
START
IS α ≷ 1 ?
α < 1
α = 1
α > 1
SET
β = MAX. No. LOOPS
n = MAX. No. ITERATIONS
SRCH TO DEGREE OF SEARCH
ENTER SRCH TO EXECUTE ONE ITERATION (S_0, P_1, P_2, ... S_1)
ENTER TRAJ TO COMPUTE THE REQUIRED NUMBER OF TRAJECTORIES
IS SEARCH 1. CONVERGED 2. CONVERGING 3. DIVERGING ?
1
2
3
END OF SEARCH
USE THE INITIAL CONDITIONS OF S_1 FOR THE NEW NOMINAL TRAJECTORY S_0
IS THE NUMBER OF LOOPS EXHAUSTED ?
YES
NO
RETURN FOR NEXT JOB
SET SUBROUTINE NOPAR TO COMPUTE A NOMINAL TRAJECTORY, SKIP RECOMPUTING PARTIAL MATRIX AND DO UP TO n ITERATIONS ON AN EXTRAPOLATED PARTIAL MATRIX
SET SUBROUTINE NOPAR TO SKIP COMPUTING A NOMINAL TRAJECTORY AND PARTIAL MATRIX, AND DO UP TO n ITERATIONS USING THE LAST PARTIAL MATRIX COMPUTED
ENTER SUBROUTINE NOPAR TO COMPLETE n ITERATIONS
ENTER TRAJ TO COMPUTE THE REQUIRED NUMBER OF TRAJECTORIES
IS SEARCH 1. CONVERGED 2. CONVERGING 3. DIVERGING ?
1
2
3
END OF SEARCH
IS THE NUMBER OF ITERATIONS EXHAUSTED ?
YES
NO
USE THE INITIAL CONDITIONS OF THE NEXT-TO-THE-LAST TRAJECTORY FOR THE NEW NOMINAL TRAJECTORY S_0
USE THE INITIAL CONDITIONS OF THE LAST TRAJECTORY FOR THE NEW NOMINAL TRAJECTORY S_0

Fig. A-1. Search procedure

II. EXTRAPOLATION PROCEDURES

A. On Initial Conditions

Define a case to be that sequence of events which results in a converged set of F_i. It is now possible to execute a series of cases (call this a job) by incrementing one of the variables used in the calculations by a constant delta until a maximum value of that variable is exceeded. This necessitates determining a set of x_{is} to start each successive case. The x_i to start case 1 must be known. Case 2 may be known, or the converged conditions of case 1 may be used as the starting x_{is} for case 2. Case 3 may be known, or the converged conditions of cases 1 and 2 are extrapolated linearly to give x_{is} for starting case 3. Once case 3 is converged, the converged conditions from cases 1, 2, and 3 are saved, and one of two paths may be followed. Either a linear extrapolation using cases 2 and 3 is used, or a quadratic extrapolation using cases 1, 2, and 3 is used to obtain x_{is} for starting case 4. The procedure, then, is to save the converged conditions of the last two or three cases and continually extrapolate to the next x_{is} until the maximum value of the variable being incremented is exceeded. Thus, at the most, it is necessary to know only the conditions x_{is} for the first three cases. Dropping the subscript i and writing the vector $\mathbf{x}$ in place of x_i,

$$\mathbf{x}_{n+1} = 2\mathbf{x}_n - \mathbf{x}_{n-1} \quad \text{(linear extrapolation)} \qquad \text{(A-4)}$$

$$\mathbf{x}_{n+1} = a_1\mathbf{x}_n - a_2\mathbf{x}_{n-1} + a_3\mathbf{x}_{n-2} \quad \text{(quadratic extrapolation)} \qquad \text{(A-5)}$$

The subscript n represents the converged point of the current case. The coefficients a_1, a_2, a_3 may be varied. Nominally, two sets are used: (1) 2.5, -2.0, 0.5 and (2) 3, -3, 1.

B. On the Partial Matrix

It is also expedient from the standpoint of real machine time consumed to perform quadratic extrapolation of the elements of the partial matrix. In order to accomplish this, it is necessary to save the partial matrices of the first three cases. Using Eq. (A-5), it is then possible to extrapolate a partial matrix for the fourth case element by element. If this is done, it is necessary only to compute the Z_{s0} of the first loop and check for convergence. If convergence is not attained, the looping procedure described is completed. The matrix elements used for the extrapolation are the elements of the last three *computed* partial matrices that give convergence. Thus, a table containing these three sets of elements is continually updated, and a partial matrix for the succeeding case may be extrapolated.